

## BMS-936564/MDX-1338: A Fully Human Anti-CXCR4 Antibody Induces Apoptosis *In Vitro* and Shows Antitumor Activity *In Vivo* in Hematologic Malignancies

Michelle R. Kuhne<sup>1</sup>, Tanya Mulvey<sup>1</sup>, Blake Belanger<sup>1</sup>, Sharline Chen<sup>1</sup>, Chin Pan<sup>1</sup>, Colin Chong<sup>1</sup>, Fei Cao<sup>1</sup>, Wafa Niekro<sup>2</sup>, Tom Kempe<sup>2</sup>, Karla A. Henning<sup>3</sup>, Lewis J. Cohen<sup>4</sup>, Alan J. Korman<sup>3</sup>, and Pina M. Cardarelli<sup>1</sup>

### Abstract

**Purpose:** CXCR4 has been identified as a prognostic marker for acute myeloid leukemia (AML) and other malignancies. We describe the development and characterization of a fully human antibody to CXCR4 and its application for therapy of AML, non-Hodgkin lymphoma (NHL), chronic lymphoid leukemia (CLL), and multiple myeloma.

**Experimental Design:** Human transgenic mice were immunized with CXCR4-expressing cells, and antibodies reactive with CXCR4 were analyzed for apoptosis induction and ability to interfere with CXCL12-induced migration and calcium flux. *In vivo* efficacy was determined in multiple AML, NHL, and multiple myeloma xenograft tumors in severe combined immunodeficient mice.

**Results:** BMS-936564/MDX-1338 is a fully human IgG<sub>4</sub> monoclonal antibody that specifically recognizes human CXCR4. *In vitro* studies show that MDX-1338 binds to CXCR4-expressing cells with low nanomolar affinity, blocks CXCL12 binding to CXCR4-expressing cells, and inhibits CXCL12-induced migration and calcium flux with low nanomolar EC<sub>50</sub> values. When given as monotherapy, MDX-1338 exhibits antitumor activity in established tumors including AML, NHL, and multiple myeloma xenograft models. In addition, we show that MDX-1338 induced apoptosis on a panel of cell lines and propose that antibody-induced apoptosis is one of the mechanisms of tumor growth inhibition.

**Conclusions:** BMS-936564/MDX-1338 is a potent CXCR4 antagonist which is efficacious as monotherapy in tumor-bearing mice and is currently in phase I for the treatment of relapsed/refractory AML, NHL, CLL, and multiple myeloma. *Clin Cancer Res*; 19(2); 357–66. ©2012 AACR.

### Introduction

CXCR4, also known as CD184, is a 7-transmembrane spanning protein consisting of an extracellular N-terminal tail and 3 extracellular loops. The intracellular carboxy terminus of CXCR4 is coupled to a heterotrimeric G-protein consisting of  $\beta$ - and  $\gamma$ -subunits and a pertussis toxin-sensitive Gi  $\alpha$ -subunit (1). To date, only one ligand for CXCR4, CXCL12, also known as SDF-1 has been identified (2, 3). CXCL12 binding to CXCR4 stimulates activation of phospholipase C and subsequently results in an elevation of cytosolic-free calcium. Ligation of CXCR4 ultimately leads to induction of chemotaxis and migration (4, 5). CXCR4 is

found in various tissues with predominant expression on hematopoietic lineage cells including B and T cells, monocytes, macrophages, natural killer (NK), and dendritic cells, as well as CD34<sup>+</sup> bone marrow progenitor cells (6). Low levels of CXCR4 are also expressed on endothelial and epithelial cells, astrocytes, and neurons (7, 8). CXCL12 has been shown to induce endothelial cell migration and proliferation and together with VEGF was shown to enhance neoangiogenesis (9).

Overexpression of CXCR4 has been found in 75% of cancers including leukemias, lymphomas, pancreatic, breast, ovarian, lung, prostate, and colorectal tumors. In addition, this pathway is implicated in stimulating the metastatic process in multiple neoplasms (10). In clinical studies, CXCR4 has been associated with increased propensity for metastasis and decreased survival and was identified as a prognostic indicator for acute myeloid leukemia (AML), breast, colorectal, non-small cell lung, ovarian, and pancreatic carcinoma in which greater expression of CXCR4 correlates with disease severity (11–16).

Bone marrow stromal cells secrete CXCL12, and the interaction with CXCR4 is essential for homing and

**Authors' Affiliations:** <sup>1</sup>Department of Cell Biology and Physiology, BDC, Bristol-Myers Squibb; Departments of <sup>2</sup>Hybridoma and <sup>3</sup>Discovery Research, BDC, Redwood City, California; and <sup>4</sup>Discovery Medicine and Clinical Pharmacology, Bristol-Myers Squibb, Lawrenceville, New Jersey

**Corresponding Author:** Pina M. Cardarelli, Bristol-Myers Squibb, 700 Bay Road, Redwood City, CA 94063. Phone: 650-260-9584; Fax: 408-545-5912; E-mail: pina.cardarelli@bms.com

doi: 10.1158/1078-0432.CCR-12-2333

©2012 American Association for Cancer Research.

### Translational Relevance

Expression of CXCR4 has been identified as a prognostic indicator for acute myeloid leukemia (AML) and other malignancies, in which greater expression of CXCR4 correlates with disease severity. CXCR4 plays an important role in both homing and retention of leukemic or stem cells in the bone marrow, and an antagonist of CXCR4 mobilizes these cells into the bloodstream. In addition to mobilization, a direct apoptotic effect of the antibody was discovered, suggesting that direct killing may be a mechanism for tumor growth inhibition. These features, together with the fact that an antibody has a longer half-life, may offer advantages over a small molecule. Consequently, clinical trials in relapsed/refractory AML, non-Hodgkin lymphoma (NHL), chronic lymphoid leukemia, and multiple myeloma are currently ongoing.

maintaining hematopoietic stem cells within the bone marrow microenvironment (17). Leukemic cells express high levels of CXCR4, and the pathway plays a critical role in leukemic cell migration into the bone marrow which in turn supports their growth and survival. CXCR4 is essential for metastatic spread to organs such as bone marrow where CXCL12 is expressed. Collectively, CXCR4 plays an important role in both homing and retention of hematopoietic stem cells in the bone marrow, and an antagonist of CXCR4 mobilizes stem cells into the bloodstream, as shown with the small-molecule CXCR4 antagonist, plerixafor (Mozobil) which was approved by the U.S. Food and Drug Administration for use in combination with granulocyte colony-stimulating factor for autologous transplants in patients with non-Hodgkin lymphoma (NHL) and multiple myeloma (18).

In AML, CXCR4 is highly expressed on the CD34<sup>+</sup> fraction of bone marrow cells. Lower levels of CXCR4 on AML cells correlate with a better prognosis resulting in a longer relapse-free and overall survival. The lower CXCR4 receptor expression attenuates migration of primary AML cells toward CXCL12 expressed in the chemoprotected environment of the bone marrow (19). In addition to AML, serum levels of CXCL12 are elevated in patients with multiple myeloma, and CXCR4 expression increases in extramedullary plasmacytoma, a manifestation of an advanced stage of multiple myeloma. Furthermore, blockade of the CXCL12/CXCR4 axis attenuates tumor growth in multiple myeloma tumor models (20).

In this report, we describe the generation of a fully human monoclonal antibody specific for human CXCR4. MDX-1338 has low nanomolar affinity for CXCR4 and effectively blocks CXCL12 binding to CXCR4, thereby inhibiting calcium flux and migration. MDX-1338 induces apoptosis on a panel of tumor cell lines and significantly reduces *in vivo* tumor growth in several xenograft models. These data

support the development of MDX-1338 for treatment of patients with hematologic malignancies.

### Materials and Methods

#### Materials

Isotype control antibody IgG<sub>4</sub> containing the S228P hinge mutation to reduce half-antibody formation (21) was produced at Medarex (acquired by BMS and currently renamed BDC). The following reagents were purchased: CXCL12 from Peprotech; <sup>125</sup>I-CXCL12 from PerkinElmer; calcium dye (FLIPR Calcium 4 kit) from Molecular Devices; bis-(acetoxymethyl)-2,2':6',2''-terpyridine-6,6''-dicarboxylate (BADTA) chemiluminescent migration reagent and DELFIA Europium solution from PerkinElmer; Annexin V Binding Buffer 10× concentrate, 7-aminoactinomycin D (7-AAD), and Annexin V-APC from BD Biosciences; phycoerythrin (PE)-conjugated goat anti-human antibody from Jackson ImmunoResearch (Cat. 109-116-098). AML peripheral blood mononuclear cells (PBMC) from AllCells LLC and Cureline Inc.

#### Cells

Ramos human B lymphoblast Burkitt lymphoma (Cat. CRL-1596), CCRF-CEM human T lymphoblast acute lymphoblastic leukemia (CCL-119), HL-60 human promyeloblast (CCL-240), Namalwa human B lymphoblast Burkitt lymphoma (CRL-1432), Raji human B lymphoblast Burkitt lymphoma (CCL-86), RPMI-8226 human myeloma (CCL-155), MM.1S human B lymphoblast MM (CRL-2974), U226B1 human myeloma (TIB-196), MV-4-11 human biphenotypic B myelomonocytic leukemia (CRL-9591), MJ human T-cell lymphoma (CRL-8294), HH human T-cell lymphoma (CRL-2105), HuT78 human lymphoblast cutaneous lymphoma (TIB-161), and NK92 human NK cell non-Hodgkin lymphoma (CRL-2407) cell lines were purchased from American Type Culture Collection (ATCC).

Nomo-1 human AML (ACC 542), MOLP-8 multiple myeloma (ACC 569), SU-DHL6 human B-cell NHL (ACC 572), L540 human Hodgkin lymphoma (ACC 72), KG-1 human AML (ACC 14), MOLP-8 human multiple myeloma (ACC 569), OPM-2 human multiple myeloma (ACC 50), and L-363 human plasma cell leukemia (ACC 49) cell lines were purchased from DSMZ.

R1610 hamster fibroblasts (CRL-1657) purchased from ATCC were transfected with human CXCR4 and kept under selection using G418 at 500 µg/mL. JJN-3 cells (ACC 541) purchased from DSMZ were selected at BMS for resistance to bortezomib. NKL human NK cell large granulocyte leukemia cell line licensed from Dana-Farber Cancer Institute (Boston, MA) and KHYG-1 human NK cell leukemia cell line (JCRB0156) was purchased from the Health Science Research Resources Bank, Japan Health Sciences Foundation.

#### FACS instrument and software

A FACSAArray or FACSCalibur (BD Biosciences) instrument and FlowJo software v8 (TreeStar Inc.) were used to collect and analyze data.

### Antibody generation

Mice from Medarex KM transgenic mouse colonies were immunized with human CXCR4 transfected R1610 cells or recombinant CXCL12. Spleen lysates were pooled and processed as described previously (22) Using proprietary phage display procedures, Biosite generated antibody fragments (Fab library). Phage which bound to CXCR4 were selected on CXCR4 magnetic proteoliposomes (MPL; ref. 23) which were prepared from HEK293E cells expressing CXCR4. Phage binding to CXCL12 was selected using biotinylated CXCL12. Selected antigen-reactive Fab were converted to full-length IgG<sub>4</sub> (S228P) and reexpressed in CHO cells.

### Functional characterization of CXCL12 and CXCR4

Serial dilutions of MDX-1338, anti-CXCL12, and control antibody were tested for blockade of <sup>125</sup>I-CXCL12 binding to CXCR4<sup>+</sup> CEM cells. Competition of <sup>125</sup>I-CXCL12 binding to CXCR4 on CEM cells was shown using a fixed concentration of <sup>125</sup>I-CXCL12 (100 pmol/L) and a titration of MDX-1338 from 5 pmol/L to 300 nmol/L. An isotype antibody was used as a negative control, and unlabeled CXCL12 was used as a positive control. Plates were incubated at room temperature for 1 hour, the filters were washed, removed, and counts per minute (CPM) were read by a PerkinElmer Wizard gamma counter. For all *in vitro* studies, the data were graphed and analyzed with GraphPad Prism software, using nonlinear regression and sigmoidal dose-response curves.

Cells were loaded with FLIPR Calcium 4 dye (Molecular Devices). A fixed concentration of CXCL12 was used to stimulate calcium flux. A titration of MDX-1338 or anti-CXCL12 from 50 pmol/L to 100 nmol/L was used to inhibit the response. A maximal calcium response was set with CXCL12 minus antibodies. A baseline response was established with buffer stimulation of cells without CXCL12. Calcium fluxes were read on the Flexstation (Molecular Devices).

Cells were loaded with BATDA. A fixed concentration of CXCL12 was used to stimulate migration of cells through a filter containing 5-μm pores on migration plates from Neuro Probe (Cat. ChemoTx 106-5). A titration of MDX-1338 or anti-CXCL12 from 20 pmol/L to 300 nmol/L was added to the cells. CXCL12 without antibody was used to establish maximal migration. Migration toward media alone without CXCL12 was used to measure background migration. Following 2-hour incubation at 37°C, migrated cells were detected by addition of Europium solution to the lysed cells and detected by time resolved fluorescence on the Fusion (Perkin Elmer).

For proliferation, cells were suspended at 1 × 10<sup>5</sup> cells/mL in growth media and incubated with antibodies and cultured for 72 hours at 37°C. Cell-Titer-Glo (Promega) was added to wells, mixed, and incubated at room temperature for 10 minutes. Plate was read on GloMax Luminometer (Promega).

For apoptosis assays, cells (5 × 10<sup>5</sup> cells/mL) were incubated with 10 to 330 nmol/L MDX-1338 or isotype control

at 37°C for 24 hours. For a subset of cells (see Table 1), a cross-linking antibody (goat anti-human IgG Fc-specific polyclonal Ab) was added at 6-fold excess. For all cell types, camptothecin (CPT) was added at 10 μmol/L for 24 hours at 37°C as a positive control for apoptosis induction. Cells were then resuspended in Annexin V binding buffer (10 mmol/L HEPES at pH 7.4, 140 mmol/L NaCl, 2.5 mmol/L CaCl<sub>2</sub>) and stained with Annexin V-APC and 7-AAD or

**Table 1.** Apoptosis data on a panel of cell lines

Cell line	Cell type	CXCR4 expression <sup>b</sup>	Adjusted percent apoptosis
Ramos <sup>a</sup>	Lymphoma	++++	71
Namalwa <sup>a</sup>	Lymphoma	++++	30
Raji <sup>a</sup>	Lymphoma	++++	15
DHL6 <sup>a</sup>	Lymphoma	+	3
L540 <sup>a</sup>	Lymphoma	+++	35
HL-60	AML	++	31
Nomo-1	AML	++++	34
KG-1	AML	++	8
MOLP-8	MM	++	19
RPML-8226	MM	++	17
MM.1S	MM	+	15
U226	MM	+	22
JJN-3R	MM	++	31
OPM2	MM	++	17
L-363	MM	+	16
MV-4-11	MM	++	1
MJ	TCL	++	9
HH	TCL	+++	9
HuT78	TCL	+	22
CCRF-CEM <sup>a</sup>	ALL	+++	45
NKL	NK	+++	36
KHYG-1	NK	+	10
NK-92	NK	++	48
Human primary <sup>a</sup>	B (CD19+)	++	17
Human primary <sup>a</sup>	T (CD3+)	+	6
Human primary <sup>a</sup>	Monocytes (CD14+)	++	24

NOTE: Cells were incubated with 10 to 330 nmol/L MDX-1338 or isotype control at 37°C for 24 hours. For a subset of cells, a cross-linking antibody (goat anti-human IgG Fc-specific polyclonal Ab) was added at 6-fold excess. Cells were then resuspended in Annexin V binding buffer and stained with Annexin V-APC and 7-AAD or PI. Cells were then washed, resuspended in Annexin V binding buffer, and analyzed with a FACSArray system and FlowJo software.

Abbreviations: MM, multiple myeloma; TCL, T-cell lymphoma.

<sup>a</sup>Without cross-linker.

<sup>b</sup>CXCR4 expression key: MFI with 10 nmol/L Ab (Score: +); 400–2000 (+); 2,000–10,000 (++); 10,000–50,000 (+++); 50,000–250,000 (++++).

propidium iodide (PI). Cells were then washed, resuspended in Annexin V binding buffer, and analyzed with a FACSArray system (BD Biosciences) and FlowJo software (TreeStar, Inc.).

### Tumor models

Severe combined immunodeficient (SCID) mice were subcutaneously implanted with 10 million Ramos cells or HL-60 cells, 7.5 million of Nomo-1 cells, 2.5 million MOLP-8 cells, or 5 million JJN-3R cells in 0.1 mL PBS and 0.1 mL Matrigel using a 1—cm<sup>3</sup> syringe and a 25-gauge half-inch needle. One day before dosing, mice were randomized into groups of 8 to 10 mice each according to tumor volume ( $L \times W \times H/2$ ). After implantation, mice were dosed with MDX-1338 at 3 to 30 mg/kg intraperitoneally (i.p.), human IgG<sub>4</sub> isotype (15 or 30 mg/kg i.p.), bortezomib (1.0 or 0.8 mg/kg i.v.), and vehicle control was dosed at 0.3 mL i.p.. Mice were dosed every 3 to 4 days for 5 doses. Tumors and body weights were measured twice weekly. Tumors were measured in 3 dimensions with a Fowler Electronic Digital Caliper (Model 62379-531; Fred V. Fowler Co.), and data were electronically recorded using StudyDirector software from Studylog Systems, Inc. Animals were checked daily for postural, grooming, and respiratory changes, as well as

lethargy. Mice were euthanized when the tumors reached the 2,000 mm<sup>3</sup> endpoint or appeared ulcerated. All antibody doses were well tolerated, and no body weight losses were observed.

### Results

#### CXCR4 is expressed on multiple hematopoietic cell lines and variably expressed in AML patients

A number of CXCR4-positive human cell lines were evaluated for MDX-1338-binding using flow cytometry. Dose-dependent binding was seen for the cell lines R1610-huCXCR4, Ramos, CEM, Nomo-1, HL-60, MOLP-8, and JJN-3R (Fig. 1). No binding to the R1610 parental cells was detected. On the basis of geometric mean fluorescent intensity (GMFI), CXCR4 levels were highest on R1610-huCXCR4 and Ramos cells followed by CEM (Fig. 1B), Nomo-1, and HL-60 (Fig. 1A). The multiple myeloma cell lines MOLP-8 and JJN-3R expressed the lowest number of receptors (Fig. 1C). The EC<sub>50</sub> values for binding were 2.3, 4.2, 10.3, 40, 5.3, 6.5, and 2.0 nmol/L for R1610-huCXCR4, Ramos, CEM, Nomo-1, HL-60 MOLP-8, and JJN-3R cells, respectively. In addition, MDX-1338 bound to healthy donor PBMCs (data not shown) as well as 7 of 8 PBMCs samples collected from patients with AML with variable GMFI (Fig. 1D).

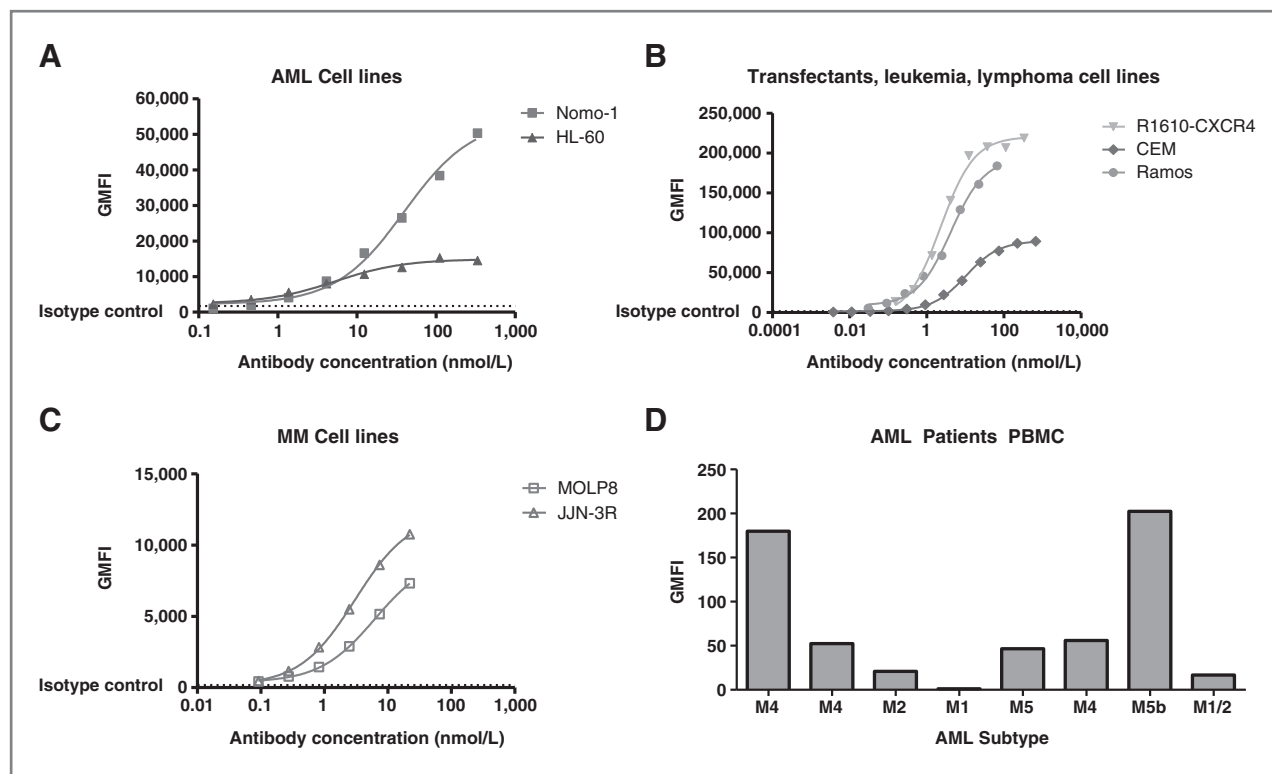


**Figure 1.** Flow cytometric analysis of MDX-1338 binding. MDX-1338 binds to AML cell lines Nomo-1 and HL-60 (A); CXCR4-transfected R1610 cells, CEM, and Ramos (B); multiple myeloma (MM) cell lines, JJN-3R and MOLP-8 (C); and primary AML patient blood cells (D). Cells were prepared for flow cytometry (FACS) staining by suspending cells with the indicated concentrations of naked MDX-1338 or biotinylated MDX-1338 before incubating the mixture of antibody and cells with goat anti-human FCγ-PE or PE-conjugated streptavidin. Cells were analyzed by FACS by gating on the live cell population identified by forward scatter (FSC) and side scatter (SSC).

### Ligand blockade

Saturation-binding studies were conducted using radiolabeled CXCL12 and CXCR4<sup>hi</sup> CEM cells. The  $K_D$  of <sup>125</sup>I-CXCL12 binding to CEM cells was determined to be 4.3 nmol/L (data not shown) which is similar to the reported  $K_D$  of CXCL12 for CXCR4 ranging from 3.0 to 5.4 nmol/L (24). Using a suboptimal fixed concentration of <sup>125</sup>I-CXCL12 (100 pmol/L), MDX-1338 was titrated, and dose-dependent inhibition of <sup>125</sup>I-CXCL12 binding with an  $EC_{50}$  value of approximately 2 nmol/L was observed (Fig. 2A). Interestingly, the anti-CXCL12 antibody was more potent and induced a dose-dependent inhibition of <sup>125</sup>I-CXCL12 binding to CEM

cells with an  $EC_{50}$  value of approximately 90 pmol/L (Fig. 2B).

### Blockade of CXCL12-induced calcium flux

Ramos and CEM cells were used to test the capacity for MDX-1338 and anti-CXCL12 to inhibit calcium flux. CXCL12 induces a dose-dependent increase in intracellular calcium with peak calcium flux reached at 50 and 5 nmol/L with Ramos and CEM cells, respectively. Using the optimal concentration of CXCL12 to stimulate calcium flux, a titration of MDX-1338 or anti-CXCL12 was used to inhibit the response (Fig. 2C and D). Both MDX-1338 and anti-CXCL12 blocked CXCL12-induced calcium flux in a dose-

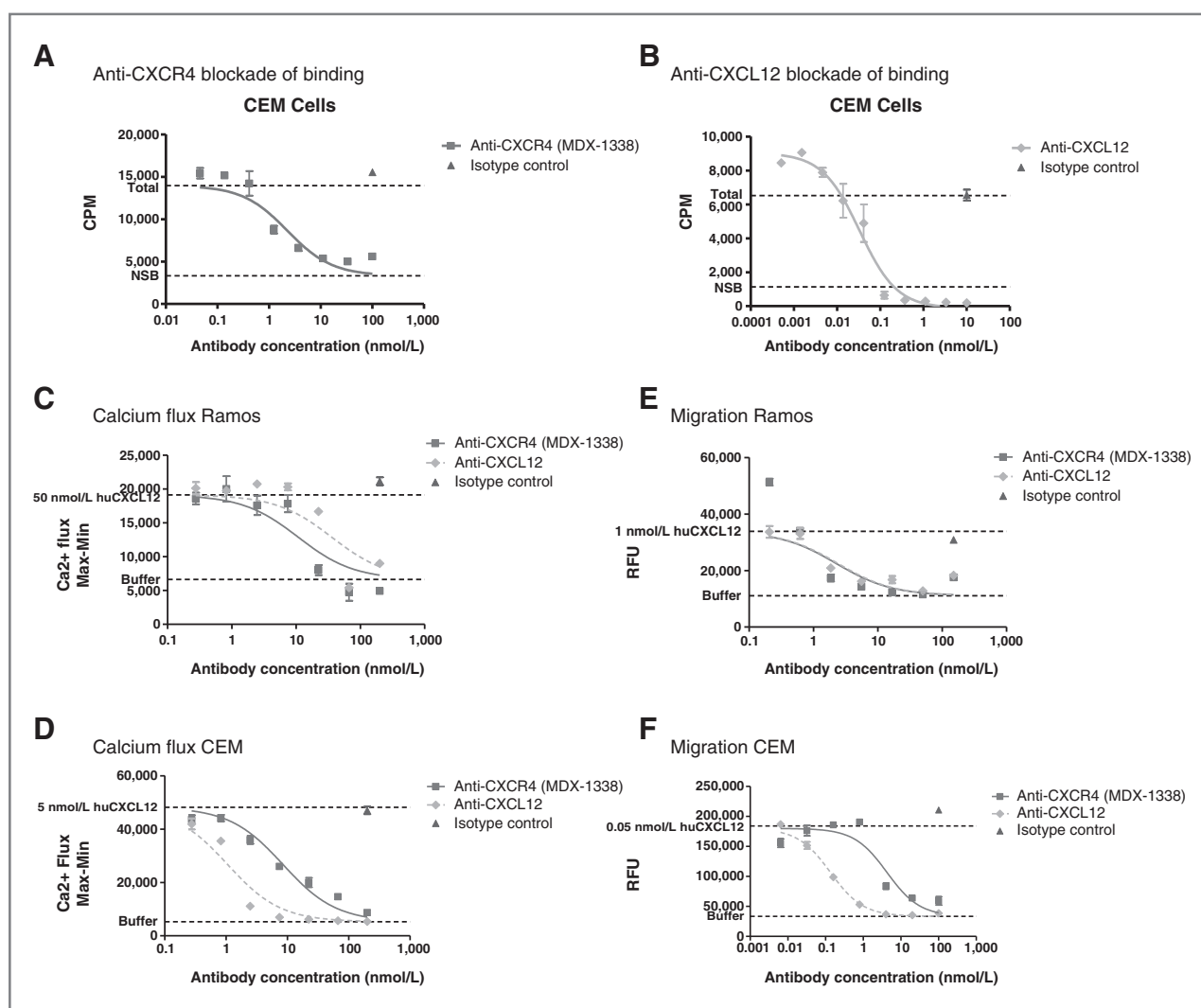


**Figure 2.** MDX-1338 blocks CXCL12 binding and cell signaling effects. Ligand binding (A and B) assays were conducted by incubating 100 pmol/L <sup>125</sup>I-CXCL12 with Ramos cells in the presence of increasing concentration of MDX-1338 (■), anti-CXCL12 antibody (◆), or isotype control antibody (▲). Unlabeled CXCL12 was added at 1,000-fold molar excess (100 nmol/L) to establish nonspecific binding (NSB). <sup>125</sup>I-CXCL12 without antibody or unlabeled competitor was added to establish total achievable binding (Total). Calcium flux assays were conducted by incubating either Ramos cells (C) or CEM cells (D) with Calcium 4 ± MDX-1338 or an isotype control. Dye-loaded cells were incubated at room temperature with 50 and 5 nmol/L CXCL12, with Ramos cells and CEM, respectively. The area under the curve of fluorescence between 20 and 200 seconds was quantitated, and an  $EC_{50}$  was calculated. Migration assays with Ramos (E) and CEM (F) cells were conducted in the presence of 1.25 and 0.05 nmol/L CXCL12, respectively. The number of labeled cells, which had migrated into the lower compartment, was measured on a Fusion (PerkinElmer) plate reader. Each point represents  $n = 3$ .

dependent manner with an  $EC_{50}$  of approximately 10 and 8 nmol/L in Ramos and CEM, respectively (Fig. 2C and D). Anti-CXCL12 blocked with an  $EC_{50}$  of approximately 35 nmol/L (Ramos) and 2 nmol/L (CEM) cells (Fig. 2C and D).

### Blockade of CXCL12-induced migration

The optimal concentration of CXCL12 for inducing Ramos migration was established to be 10 ng/mL (1.25 nmol/L), whereas CEM cells were more sensitive to CXCL12 and exhibited maximal migration at 0.05 nmol/L CXCL12. MDX-1338 was shown to block CXCL12-induced migration with an approximate  $EC_{50}$  value of 1 nmol/L in Ramos cells and 4 nmol/L in CEM cells (Fig. 2E and F). Anti-CXCL12 inhibited CXCL12-induced migration with an approximate  $EC_{50}$  value of 0.9 nmol/L (Ramos) and 0.13 nmol/L (CEM) cells (Fig. 2E and F).

### Comparison of anti-CXCR4 and anti-CXCL12 antibodies *in vivo*

To test the *in vivo* activity of MDX-1338 and anti-CXCL12, SCID mice bearing established Ramos tumor xenografts were treated with 15 mg/kg of antibody. Dose-response studies had previously found 15 mg/kg to be an effective dose of rituximab (data not shown). MDX-1338 and positive control, rituximab, inhibited tumor growth when compared with vehicle and isotype controls. Treatment with MDX-1338 resulted in a median growth inhibition of 99% on day 21, and the inhibition was maintained for 60 days (Fig. 3A). In contrast, anti-CXCL12 did not inhibit tumor growth and did similarly to the isotype control antibody.

### *In vitro* induction of apoptosis

Because we observed robust *in vivo* activity, studies were undertaken to understand the mechanism of action of MDX-1338. A maximum of about 50% inhibition of Ramos cell proliferation was seen with 40 nmol/L MDX-1338 treatment (Fig. 4A) compared with isotype control. By comparison, AMD3100, a small-molecule CXCR4 antagonist did not inhibit proliferation. A recently described peptide antagonist, BKT140, did inhibit proliferation, however, at much higher concentrations (100  $\mu$ mol/L).

Antibody-induced apoptosis was investigated using Ramos cells and MDX-1338 for 24 hours. For comparison, the small-molecule CXCR4 antagonist, AMD3100, was investigated using 6  $\mu$ mol/L corresponding to a concentration which inhibited CXCL12-induced calcium flux and migration. MDX-1338 induced an increase in Annexin V (31.2%) and in Annexin V/PI double-positive staining (27.3%) compared with cells that were untreated (1.7% and 4.1%), incubated with isotype control antibody (0.5% and 2.8%), or treated with AMD3100 (2.0% and 2.7%; Fig. 4B and C).

To verify the specificity of the response to MDX-1338, parental R1610 which do not bind MDX-1338 (data not shown) and R1610 transfected with human CXCR4 that do bind to MDX-1338 (Fig. 1) were used to measure apoptosis. The transfected cells R1610-hCXCR4 exhibited an increased level of Annexin V staining and Annexin V/PI in response to

incubation with MDX-1338 (24.3% and 11.4%), whereas an isotype control antibody (2.5% and 0.9%) or when untreated (2.6% and 0.9%) had minimal effects. The parental R1610 cells did not exhibit apoptosis following MDX-1338 treatment (Fig. 5) suggesting specificity for hCXCR4. Subsequent to these findings, MDX-1338 was shown to induce apoptosis on several CXCR4-positive cell lines as well as normal PBMCs (Table 1).

### MDX-1338 inhibits tumor growth of AML models

To assess the efficacy of antibody in AML, we used 2 cytarabine-resistant mouse xenograft models, HL-60 and Nomo-1. The CXCR4 expression in each cell line was confirmed by fluorescence-activated cell-sorting (FACS) staining (Fig. 1A). SCID mice containing established HL-60 tumors were treated with MDX-1338, and on day 27, the median tumor growth inhibition was 88% and 83% when compared with isotype and vehicle groups, respectively (Fig. 3B).

In the Nomo-1 model, the mice were dosed with MDX-1338 or cytarabine and monitored for 57 days. On day 34, the median tumor growth inhibition of MDX-1338-treated mice was significantly delayed by 88% compared with isotype or vehicle control (Fig. 3C). As expected, cytarabine did not inhibit tumor growth.

### MDX-1338 inhibits tumor growth of multiple myeloma models

CXCR4<sup>+</sup> myeloma cells, MOLP-8 and JJN-3R, were tested for sensitivity to MDX-1338 in SCID xenograft tumor models. MOLP-8 cells were implanted into SCID mice and the mice were treated with 10 mg/kg/dose of MDX-1338  $\pm$  50 mg/kg lenalidomide or  $\pm$ 0.8 mg/kg bortezomib (Fig. 3D). MDX-1338 significantly delayed mean tumor growth by 66% and 56% when compared with isotype control on day 25 (last day when all mice in each cohort remained in the study). MOLP-8 tumors were relatively resistant to lenalidomide and bortezomib, and the efficacy of MDX-1338 was not improved when combined with either drug. At the end of study on day 42, 5 of 8 mice remained in the MDX-1338 group, whereas no mice remained in the isotype-treated group. The bortezomib-resistant, JJN-3R cells were implanted into SCID mice, and mice were dosed when the tumors were established. Median tumor growth over time is shown in Fig. 3E. Neither lenalidomide nor bortezomib alone inhibited tumor growth, whereas median tumor growth inhibition was 100% for mice treated with MDX-1338 on day 25 compared with mice treated with isotype. At the end of study, 4 of 7 mice were tumor free in the MDX-1338 30 mg/kg group.

### Discussion

A novel, first-in-class therapeutic monoclonal antibody directed to CXCR4 has been developed. In addition to blocking CXCL12-induced calcium flux and migration, we describe antibody-dependent induction of apoptosis as another mechanism of action. Antibody-induced apoptosis resulted in robust *in vivo* efficacy across multiple

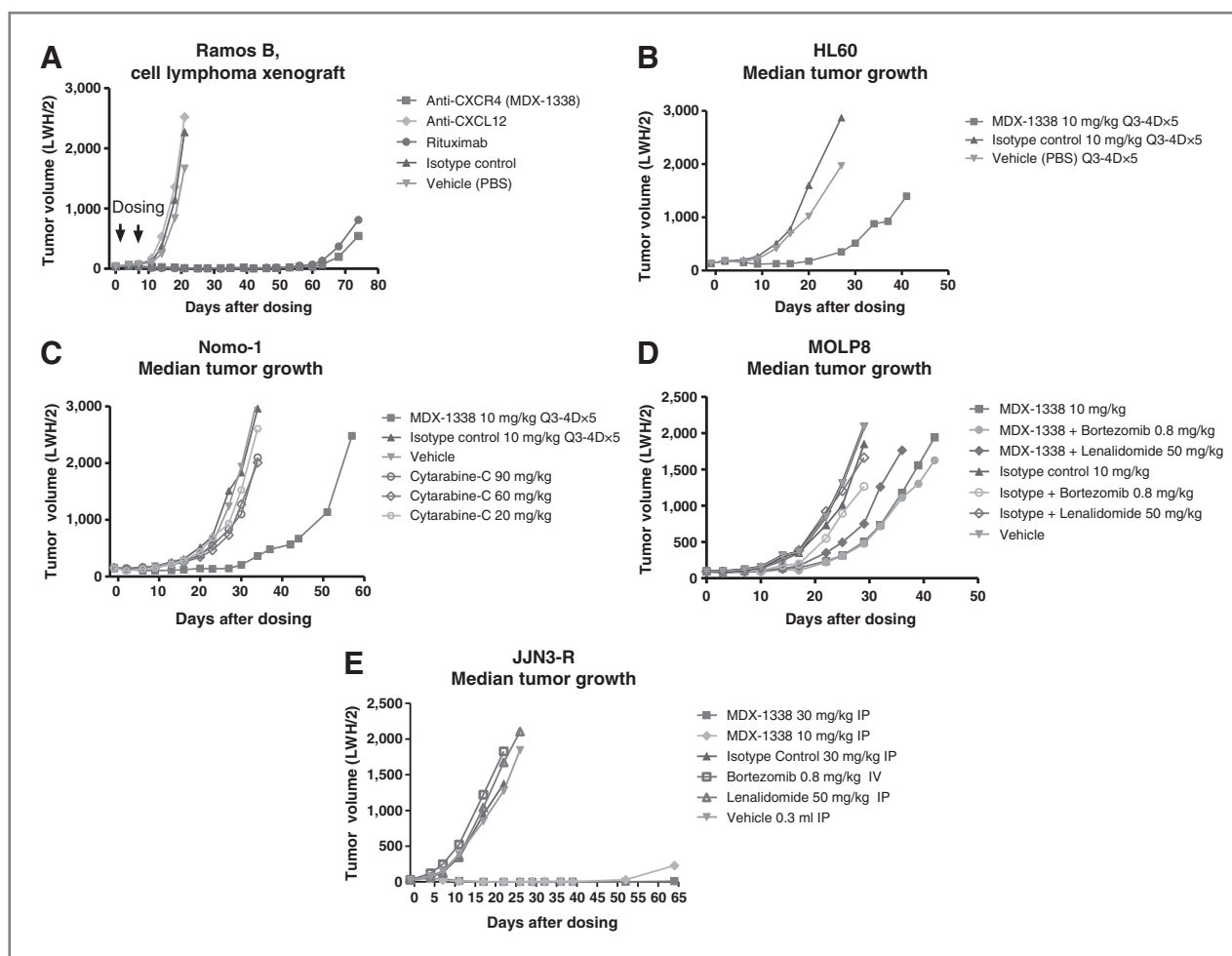


**Figure 3.** A blocking CXCR4 antibody inhibits tumor growth *in vivo*, whereas a blocking CXCL12 antibody does not inhibit tumor growth. **A**, Ramos cells were implanted subcutaneously and when a mean and median tumor size of 80 mm<sup>3</sup> was reached, the mice were randomized ( $n = 8$ ). On days 0 and 7, each animal was injected i.p. with about 200  $\mu$ L of MDX-1338 (15 mg/kg/dose), anti-CXCL12 (15 mg/kg/dose), human IgG4 isotype control (15 mg/kg/dose), rituximab (15 mg/kg/dose), or PBS (vehicle control). Tumors were measured in 3 dimensions ( $L \times W \times H/2$ ). When the tumor was at least 2,000 mm<sup>3</sup> or appeared ulcerated, animals were euthanized. **B**, HL-60 cells were implanted subcutaneously into SCID mice. When the tumor volume reached approximately 136 mm<sup>3</sup>, the mice were randomized ( $n = 10$ ) and dosed on days 0, 3, 7, 10, and 14 and monitored for 41 days. **C**, Nomo-1 cells were implanted s.c. into SCID mice. When the tumor volume reached approximately 84 mm<sup>3</sup>, the mice were randomized ( $n = 9$ ) and dosed on days 0, 3, 7, 10, and 14. **D**, MOLP-8 cells were implanted into SCID mice. When the tumor volume reached approximately 100 mm<sup>3</sup>, the mice were randomized ( $n = 8$ ) and dosed on days 0, 3, 7, 10, and 14 with MDX-1338 alone or with 50 mg/kg lenalidomide or with 0.8 mg/kg bortezomib. **E**, JJN-3R cells were implanted, and when the tumor volume reached approximately 100 mm<sup>3</sup>, the mice were randomized ( $n = 8$ ) and dosed with MDX-1338 or 50 mg/kg lenalidomide or 0.8 mg/kg bortezomib. Dosing occurred on days 0, 4, 7, 11, and 14 and was monitored for 65 days.

hematopoietic tumor xenograft models. Because CXCR4 plays a role in multiple fundamental aspects of cancer including proliferation, migration/invasion, and angiogenesis, an antagonist has potentially multiple means to intervene in malignancies where CXCR4 is expressed. To begin to dissect the pathway, we developed fully human monoclonal antibodies to both CXCR4 and CXCL12. Both the anti-CXCR4 and anti-CXCL12 antibodies inhibit ligand binding to CXCR4 resulting in inhibition of ligand-induced cellular responses such as calcium flux and migration (Fig. 2). In addition to these functions, the CXCR4/CXCL12 axis has been implicated in promoting angiogenesis (9, 25). Both anti-CXCR4 and anti-CXCL12 antibodies also inhibited endothelial tube for-

mation (data not shown), an *in vitro* demonstration of angiogenesis.

To test our theory that disruption of CXCR4/CXCL12 interactions will result in attenuation of tumor growth, we tested the efficacy of the antibodies in an *in vivo* xenograft model. Ramos cells were engrafted into SCID mice and rituximab was used as a positive control. To our surprise, anti-CXCL12 antibody did not control tumor growth and appeared indistinguishable from vehicle and isotype control. In contrast, anti-CXCR4 antibody showed nearly complete tumor growth control with similar activity as rituximab (Fig. 3). Because *in vitro* blockade of chemotaxis was similar between the 2 antibodies, it is unlikely that antitumor control is dependent on blockade of the CXCL12/

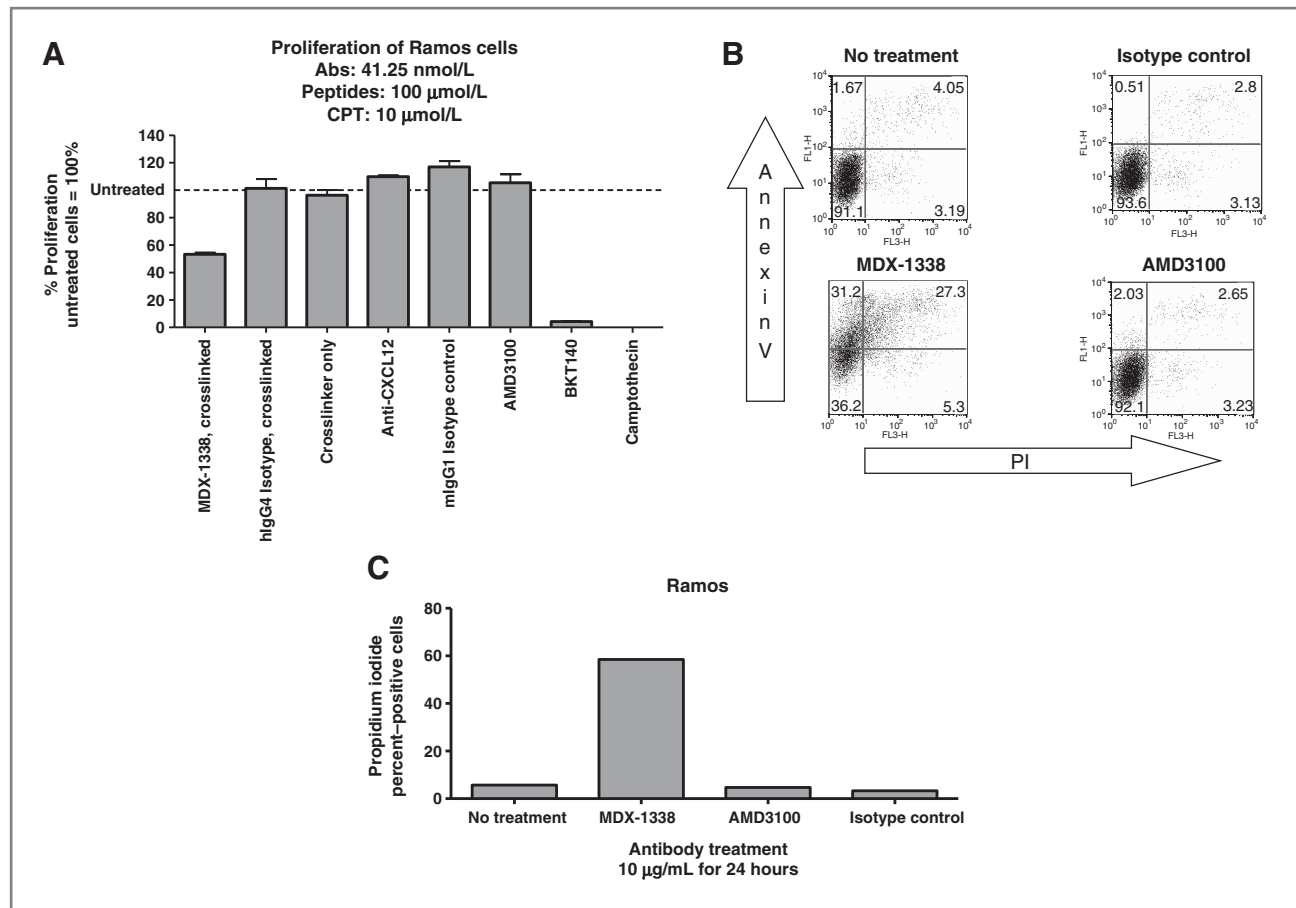


Figure 4. MDX-1338 inhibits proliferation and induces apoptosis. A, Ramos cells were cultured with MDX-1338 or isotype control antibody for a total of 72 hours. B and C, apoptotic assays were carried by incubating Ramos cells for 24 hours at 37°C with 10 μg/mL MDX-1338 or isotype control. Cells were stained with Annexin V-FITC and PI. The percentage of cells positive for Annexin V only or both Annexin V and PI double-positive was determined.

CXCR4 axis. A direct effect of MDX-1338 was tested in a Ramos cell proliferation assay. CXCL12 has been implicated as an autocrine factor promoting cell growth, and in a separate study, CXCL12 siRNA inhibited BR5-1 growth (26, 27). Although the inhibition of growth was partial

our studies, we observed a dose-dependent inhibition of proliferation with anti-CXCR4, whereas AMD3100 and anti-CXCL12 antibody had no effect. Recently, a 14-residue polypeptide reported to be a specific CXCR4 antagonist (BKT140) was shown to inhibit proliferation of multiple

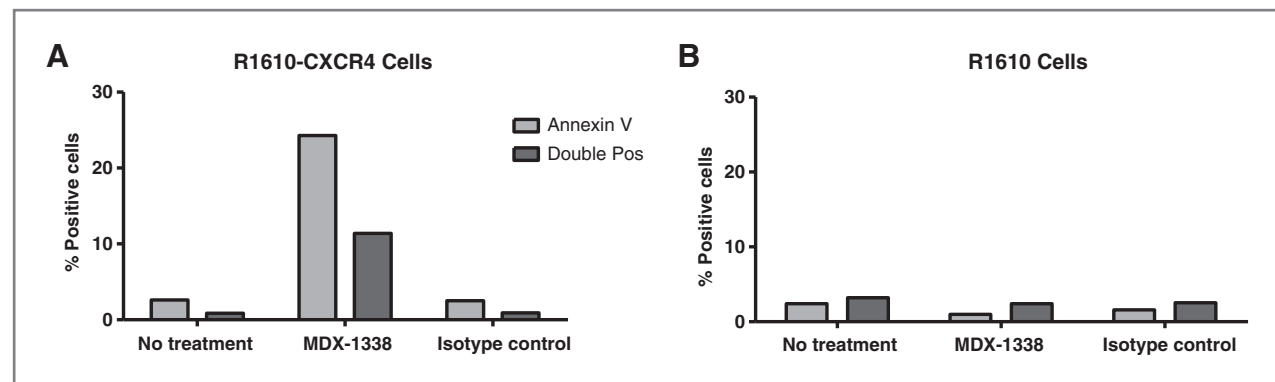


Figure 5. Induction of apoptosis by MDX-1338 is CXCR4-specific. MDX-1338 or isotype control were added to R1610 parental cells (B) and CXCR4-transfected cells (A) for 24 hours at 37°C and then stained with Annexin V-FITC and PI. The percentage of cells that are positive for Annexin V only or both Annexin V and PI double-positive was determined.



myeloma cells (28). It has been suggested that AMD3100 is a weak partial agonist, whereas BKT140 acts as an inverse agonist (29).

Multiple agents are being developed or are approved for CXCL12/CXCR4-targeted therapy including small-molecule inhibitors, AMD3100 (plerixafor, Mozobil, developed by Genzyme), BKT140 (Biokine Therapeutics; ref. 28), a cyclic peptide CXCR4 antagonist (Eli Lilly; ref. 30), and CTCE-9908 developed by Chemokine Therapeutics (31, 32). In addition, an anti-CXCR4 antibody developed by Eli Lilly has been discontinued and an antibody developed by Pierre Fabre Medicament (33) is in preclinical development. Finally, a first-in-man study of ALX-0651, a nanobody inhibiting CXCR4, was initiated in healthy volunteers by Ablynx (34). How these various therapies will be differentiated needs to be determined. We have compared the activity of AMD3100 with MDX-1338, and there was no apoptosis observed with AMD3100, suggesting that the antibody binding to CXCR4 drives a signal to induce apoptosis and is not simply antagonizing ligand binding. Our current data support that MDX-1338 activates the intrinsic apoptotic pathway. The specific signaling pathways that CXCR4 engages upon antibody binding are currently being investigated.

The observation of CXCR4-mediated apoptosis by binding of HIV-1 envelope glycoprotein-gp120 to CXCR4 has been reported (35). Investigation revealed that antibodies cross-linked to CXCR4 could mimic the cell death observed with gp120 induction (36). Those authors suggested that the use of anti-chemokine receptor antibodies to prevent HIV-1 infection might result in an efficient and rapid destruction of the receptor expressing T cells. We measured anti-CXCR4-induced apoptosis in more than 20 different CXCR4-expressing cell lines (Table 1), confirming that this mechanism is not restricted to one cell type. Although MDX-1338 binds to healthy peripheral blood leukocytes, preliminary data from our AML trial have shown that the drug is well tolerated. To date, more than 40 patients have been dosed up to 10 mg/kg, and we have not seen any adverse events associated with the antibody.

*In vivo* published data support that antagonists of CXCR4 are efficacious in AML and multiple myeloma tumor models by enhancing the sensitivity of the tumors cells to chemotherapy (37, 38). In contrast, in the studies presented here, we show that a statistically significant tumor growth

inhibition was achieved when MDX-1338 was administered as monotherapy in AML and multiple myeloma models.

As MDX-1338 is an IgG<sub>4</sub> antibody, the *in vivo* efficacy cannot be explained by antibody-dependent cell-mediated cytotoxicity (ADCC) or complement-dependent cytotoxicity (CDC). However, it is possible that the antibody, once bound to CXCR4-expressing cells, engages FcγR1 receptors expressed on antigen-presenting cells leading to phagocytosis. The cell lines, in which MDX-1338 efficacy was observed *in vivo*, required a secondary anti-Fc antibody to MDX-1338 to induce apoptosis *in vitro*. This may be a consequence of lower expression of CXCR4 on those particular cell lines. If the mechanism of apoptosis initiation is dependent upon bringing CXCR4 molecules into close proximity and the density of CXCR4 on the cell surface is low relative to the binding distance spanned by the anti-CXCR4 antibody, then a secondary high-affinity anti-Fc antibody may be required to bridge that gap, bringing the receptors together to drive an apoptotic signal. *In vivo*, this may be accomplished through FcγR1 receptors.

In conclusion, we propose a novel mechanism of action for an anti-CXCR4 antibody in addition to its role in cellular mobilization and also that MDX-1338 may be an effective therapy for AML, multiple myeloma, and other hematologic and possibly solid tumor malignancies.

#### Disclosure of Potential Conflicts of Interest

No potential conflicts of interest were disclosed.

#### Authors' Contributions

**Conception and design:** M.R. Kuhne, C. Pan, A.J. Korman, P.M. Cardarelli  
**Development of methodology:** M.R. Kuhne, B. Belanger, C. Pan, W. Niekro, K.A. Henning

**Acquisition of data (provided animals, acquired and managed patients, provided facilities, etc.):** M.R. Kuhne, T. Mulvey, B. Belanger, S. Chen, C. Chong, F. Cao, K.A. Henning

**Analysis and interpretation of data (e.g., statistical analysis, biostatistics, computational analysis):** M.R. Kuhne, T. Mulvey, B. Belanger, S. Chen, C. Pan, F. Cao, K.A. Henning, P.M. Cardarelli

**Writing, review, and/or revision of the manuscript:** M.R. Kuhne, S. Chen, C. Pan, W. Niekro, K.A. Henning, L.J. Cohen, A.J. Korman, P.M. Cardarelli

**Administrative, technical, or material support (i.e., reporting or organizing data, constructing databases):** M.R. Kuhne, T. Mulvey, W. Niekro  
**Study supervision:** M.R. Kuhne, C. Pan

**Antibody generation and discovery:** T. Kempe

The costs of publication of this article were defrayed in part by the payment of page charges. This article must therefore be hereby marked *advertisement* in accordance with 18 U.S.C. Section 1734 solely to indicate this fact.

Received July 13, 2012; revised October 10, 2012; accepted November 2, 2012; published OnlineFirst December 4, 2012.

#### References

- Loetscher M, Geiser T, O'Reilly T, Zwahlen R, Baggiolini M, Moser B. Cloning of a human seven-transmembrane domain receptor, LESTR, that is highly expressed in leukocytes. *J Biol Chem* 1994;269:232-7.
- Bleul CC, Farzan M, Choe H, Parolin C, Clark-Lewis I, Sodroski J, et al. The lymphocyte chemoattractant SDF-1 is a ligand for LESTR/fusin and blocks HIV-1 entry. *Nature* 1996;382:829-33.
- Oberlin E, Amara A, Bachelier F, Bessia C, Virelizier J.-L, Arenzana-Seisdedos F, et al. The CXC Chemokine SDF-1 is the ligand for LESTR/fusin and prevents infection by T-cell-line-adapted HIV-1. *Nature* 1996;382:833-5.
- Tachibana K, Hirota S, Iizasa H, Yoshida H, Kawabata K, Kataoka Y, et al. The chemokine receptor CXCR4 is essential for vascularization of the gastrointestinal tract. *Nature* 1998;393:591-4.
- Zou YR, Kottmann AH, Kuroda M, Taniuchi I, Littman DR. Function of the chemokine receptor CXCR4 in hematopoiesis and in cerebellar development. *Nature* 1998;393:595-9.
- Lee B, Sharron M, Montaner LJ, Weissman D, Doms RW. Quantification of CD4, CCR5 and CXCR4 levels on lymphocyte subsets, dendritic cells and differentially conditioned monocyte-derived macrophages. *Proc Natl Acad Sci U S A* 1999;96:5215-20.

7. Gupta SK, Lysko PG, Pillarisetti K, Ohlstein E, Stadel J. M. Chemokine receptors in human endothelial cells. Functional expression of CXCR4 and its transcriptional regulation by inflammatory cytokines. *J Biol Chem* 1998;273:4282-7.
8. Hesselgesser J, Halks-Miller M, DelVecchio V, Peiper SC, Hoxie J, Kolson DL, et al. CD4-independent association between HIV-1 gp120 and CXCR4: functional chemokine receptors are expressed in human neurons. *Curr Biol* 1997;7:112-21.
9. Guleng B, Tateishi K, Ohta M, Kanai F, Jazaq A, Ijichi H, et al. Blockade of the stromal cell-derived factor-1/CXCR4 axis attenuates *in vivo* tumor growth by inhibiting angiogenesis in a vascular endothelial growth factor-independent manner. *Cancer Res* 2005;65:5864-71.
10. Murphy PM. Chemokines and the molecular basis of cancer metastasis. *N Engl J Med* 2001;345:833-5.
11. Spoo AC, Lubbert M, Wierda W, Burger J. CXCR4 is a prognostic marker in acute myelogenous leukemia. *Blood* 2007;109:786-91.
12. Hiller DJ, Meschonat C, Kim R, Li BD, Chu QD. Chemokine receptor CXCR4 level in primary tumors independently predicts outcome for patients with locally advanced breast cancer. *Surgery* 2011;150:459-65.
13. Ottaviano A, Franco R, Talamanca AA, Liguori G, Tatangelo F, Delrio P, et al. Overexpression of both CXCR4 chemokine receptor 4 and vascular endothelial growth factor proteins predicts early distant relapse in stage II-III colorectal cancer patients. *Clin Cancer Res* 2006;12:2795-803.
14. Spano JP, Andre F, Morat L, Sabatier L, Besse B, Combadiere C, et al. Chemokine receptor CXCR4 and early-stage non-small cell lung cancer: pattern of expression and correlation with outcome. *Ann Oncol* 2004;15:613-7.
15. Jiang YP, Wu XH, Shi B, Wu WX, Yin GR. Expression of chemokine CXCL12 and its receptor CXCR4 in human epithelial ovarian cancer: an independent prognostic factor for tumor progression. *Gynecol Oncol* 2006;103:226-33.
16. Marechal R, Demetter P, Nagy N, Berton A, Decaestecker C, Polus M, et al. High expression of CXCR4 may predict poor survival in resected pancreatic adenocarcinoma. *Br J Cancer* 2009;100:1444-51.
17. Mohle R, Bautz F, Rafii S, Moore MA, Brugger W, Kanz L. The chemokine receptor CXCR4 is expressed on CD34+ hematopoietic progenitors and leukemic cells and mediates transendothelial migration induced by stromal cell-derived factor-1. *Blood* 1998;91:4523-30.
18. Dar A, Schajnovitz A, Lapid K, Kalinkovich A, Itkin T, Ludin A, et al. Rapid mobilization of hematopoietic progenitors by AMD3100 and catecholamines is mediated by CXCR4-dependent SDF-1 release from bone marrow stromal cells. *Leukemia* 2011;25:1286-96.
19. Tavor S, Petit I, Porozov S, Avigdor A, Dar A, Leider-Trejo L, et al. CXCR4 regulates migration and development of human acute myelogenous leukemia stem cells in transplanted NOD/SCID mice. *Cancer Res* 2004;64:2817-24.
20. Alsayed Y, Ngo H, Runnels J, Leleu X, Singha U, Pitsillides C, et al. Mechanism of regulation of CXCR4/SDF-1 (CXCL12)-dependent migration and homing in multiple myeloma. *Blood* 2007;109:2708-17.
21. Angal S, King DJ, Bodmer MW, Turner A, Lawson AD, Roberts G, et al. A single amino acid substitution abolishes the heterogeneity of chimeric mouse/human (IgG4) antibody. *Mol Immunol* 1993;30:105-8.
22. Buechler J, Valkirs G, Gray J, Lonberg Linventors; Biosite, Inc., assignee. Human antibodies. United States patent US6794132. 2004 Sep 21.
23. Mirzabekov T, Bannert N, Farzan M, Hofmann W, Kolchinsky P, Wu L, et al. Enhanced expression, native purification, and characterization of CCR5, a principal HIV-1 coreceptor. *J Biol Chem* 1999;274:28745-50.
24. Di Salvo J, Koch GE, Johnson KE, Blake AD, Daugherty BL, DeMartino JA, et al. The CXCR4 agonist ligand stromal derived factor-1 maintains high affinity for receptors in both Gai-coupled and uncoupled states. *Eur J Pharmacol* 2000;409:143-54.
25. Ping YF, Yao XH, Jiang JY, Zhao LT, Yu SC, Jiang T, et al. The chemokine CXCL12 and its receptor CXCR4 promote glioma stem cell-mediated VEGF production and tumour angiogenesis via P13K/AKT signalling. *J Pathol* 2011;224:344-54.
26. Liu Z, Stanojevic V, Avadhani S, Yano T, Habener JF. Stromal cell-derived factor-1 (SDF-1)/chemokine (C-X-C motif) receptor 4 (CXCR4) axis activation induces intra-islet glucagon-like peptide-1 (GLP-1) production and enhances beta cell survival. *Diabetologia* 2011;54:2067-76.
27. Righi E, Kashiwagi S, Yuan J, Santosuosso M, Leblanc P, Ingraham R, et al. CXCL12/CXCR4 blockade induces multimodal antitumor effects that prolong survival in an immunocompetent mouse model of ovarian cancer. *Cancer Res* 2011;71:5522-34.
28. Beider K, Begin M, Abraham M, Wald H, Weiss ID, Wald O, et al. CXCR4 antagonist 4F-benzoyl-TN14003 inhibits leukemia and multiple myeloma tumor growth. *Exp Hematol* 2011;39:282-92.
29. Zhang WB, Navenot J.-M, Haribabu B, Tamamura H, Hiramatu K, Omagari A, et al. A point mutation that confers constitutive activity to CXCR4 reveals that T140 is an inverse agonist and that AMD3100 and ALX40-4C are weak partial agonists. *J Biol Chem* 2002;277:24515-21.
30. Fetzer OS, Hwang J, Soo PL, Ng P-S, Svenson Sinventors; Cerulean Pharma Inc., assignee. Therapeutic peptide-polymer conjugates, particles, compositions, and related methods publication date. United States patent US20120052097. 2011 Aug 18.
31. Richert M, Vaidya K, Mills C, Wong D, Korz W, Hurst D, et al. Inhibition of CXCR4 by CTCE-9908 inhibits breast cancer metastasis to lung and bone. *Oncol Rep* 2009;21:761-767.
32. Porvasnik S, Sakamoto N, Kusmartsev S, Eruslanov E, Kim WJ, Cao W, et al. Effects of CXCR4 antagonist CTCE-9908 on prostate tumor growth. *The Prostate* 2009;69:1460-9.
33. Corvaia N, Berger S, Wirch T, Boute N, Broussas M, Beau-Larvor C, et al. 515H7, a novel anti-CXCR4 antibody: *in vitro* efficacy on CXCR4-associated signaling pathways and *in vivo* anti-tumor activity [abstract]. In: Proceedings of the 102nd Annual Meeting of the American Association for Cancer Research; 2011 Apr 2-6; Orlando, FL. Philadelphia (PA): AACR; 2011. Abstract nr 4571.
34. Clinical Trials.gov-NCT01374503. Available from: <http://clinicaltrials.gov/ct2/show/NCT01374503>.
35. Garg H, Blumenthal R. HIV gp41-induced apoptosis is mediated by caspase-3-dependent mitochondrial depolarization, which is inhibited by HIV protease inhibitor nelfinavir. *J Leukocyte Biol* 2006;79:351-62.
36. Berndt C, Mopps B, Angermuller S, Gierschik P, Krammer PH. CXCR4 and CD4 mediate a rapid CD95-independent cell death in CD4+ T cells. *Proc Natl Acad Sci U S A* 1998;95:12556-61.
37. Azab AK, Runnels J, Pitsillides C, Moreau AS, Azab F, Leleu X, et al. CXCR4 inhibitor AMD3100 disrupts the interaction of multiple myeloma cells with the bone marrow microenvironment and enhances their sensitivity to therapy. *Blood* 2009;113:4341-51.
38. Zeng Z, Shi Y, Samudio I, Wang RY, Ling X, Frolova O, et al. Targeting the leukemia microenvironment by CXCR4 inhibition overcomes resistance to kinase inhibitors and chemotherapy in AML. *Blood* 2009;113:6215-24.